Electronic Supplementary Information (ESI)

Enhanced Room Temperature Ionic Conductivity in the $LiBH_4 \cdot ½NH_3$-Al_2O_3 Composite

Ruixue Zhang,[a] Wanying Zhao,[b] Zhenzhen Liu,[b] Shanghai Wei,[c] Yigang Yan,*[ad] Yungui Chen,*[ad]

[a] Institute of New Energy and Low-Carbon Technology, Sichuan University Chengdu 610207, China; Email: yigang.yan@scu.edu.cn, chenyungui@scu.edu.cn
[b] College of Materials Science and Engineering, Sichuan University, Chengdu 610065, China.
[c] Department of Chemical & Materials Engineering, Faculty of Engineering, the University of Auckland, Auckland 1142, New Zealand.
[d] Engineering Research Center of Sustainable Energy Materials and Devices, Ministry of Education, China

Experimental Methods:

$LiBH_4$ (≥95%, Sigma-Aldrich), $LiNH_2$(95%, Sigma-Aldrich) and LiOH (≥98%, Sigma-Aldrich) were used directly without extra purification. γ-Al_2O_3 nanopowders (99.99%, Beijing Deke Daojin Science and Technology Co. Ltd) were dried at 350 ºC for 24 h under vacuum to remove the adsorbed water and oxygen. To synthesize $LiBH_4 \cdot ½NH_3$-Al_2O_3 composite, 1 g mixture of $LiBH_4$, $LiNH_2$, LiOH and Al_2O_3 was mechanically milled in a 50 mL sealed stainless-steel milling jar at 300 rpm for 0.5 h with a ball-to-sample mass ratio of 20:1 using a planetary ball mill (PMQ0.4L). Subsequently, the mixture was annealed at 60ºC for 20 h under Ar atmosphere. The molar ratio of $LiBH_4$, $LiNH_2$ and LiOH was fixed as 2:1:1. The addition amount of Al_2O_3 was set as 30, 45, 53, 60, 63, 67 and 75 wt% Al_2O_3, respectively. All sample

handlings were performed in an Ar-filled glovebox (MIKROUNA, China, $H_2O < 0.01$ ppm and $O_2 < 0.01$ ppm).

X-ray diffraction (XRD) measurements were carried out using Cu Kα (λ=1.5416 Å) radiation with the 2θ range of 20－70° and a scan rate of $0.026° \cdot s^{-1}$ using EMPYREAN X-ray diffractometer. Investigated powder was sealed by 3M 7413D tape to prevent the air exposure. Differential scanning calorimetry (DSC) measurements were performed using a Mettler-Toledo TGA/DSC2 instrument (N_2 flow: 50 mL min^{-1}, ramp: 5 ºC min^{-1}, temperature range: –40 to 80 ºC) and the samples were filled in Al pan in Ar-filled glovebox. Fourier-transform infrared (FTIR) spectra were collected using Thermo Fisher Nicolet iS50 ATR spectrometer with the resolution of 4 cm^{-1}. The morphologies of the samples were observed using Titan G2 transmission electron microscopy (TEM) with a vacuum transfer chamber.

The X-ray photograph spectroscopy (XPS) spectra were recorded on Thermo Scientific K-Alpha+, XPS system. The samples transfer and handing process were protected under inert gas. The binding energies of B 1s, Li 1s, N 1s, O 1s and Al 2p calibrated with C 1s peak (BE = 284.6 eV) as a standard.

Ionic conductivity was measured by electrochemical impedance spectroscopy (EIS) using Mulit Autolab M204 electrochemical workstation. Au films were used as blocking electrodes and frequency varies from 1 Hz to 1 MHz. The powder samples were pressed into pellets in diameter of 0.6 mm with thickness of ~ 1 mm under a pressure of 0.3 GPa. The temperature range for the EIS measurement was set as 30 to 80 ºC with a step of 10 ºC and dwell time of 2 h. The ionic conductivity was obtained

using the following equation

$$\sigma = \frac{d}{R\,S} \qquad (1)$$

where d is the thickness of the electrolyte, R is the resistance which is determined as the intersection of curve with the Z' axis the and S is the contact area between the electrode and electrolyte.

Cyclic voltammetry (CV) test at a scan rate of 0.5 mV s^{-1} was performed at room temperature (RT) from –0.5 to 4.0 V with a Li| $LiBH_4 \cdot ½NH_3$-Al_2O_3 |SS (SS: stainless steel) cell using an electrochemical work station (DH7000, Donghua, China). The galvanostatic plating-stripping test was conducted using an Li|$LiBH_4 \cdot ½NH_3$-Al_2O_3|Li symmetric cell at the constant current density of ±0.1 mA cm^{-2} at 30 ºC.

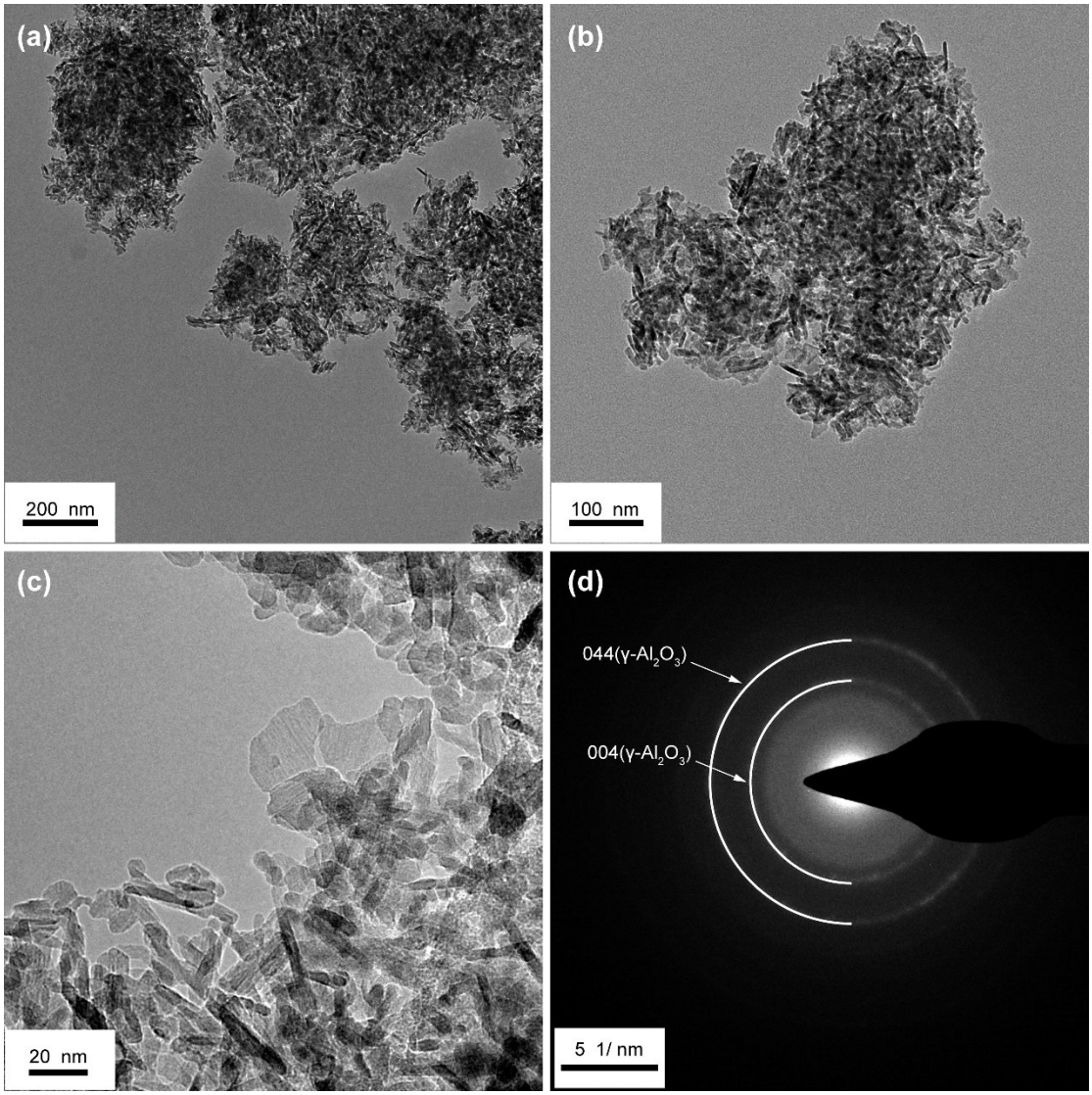

Fig. S1 (a), (b) and (c): TEM images of the γ-Al_2O_3 nanopowders; (d) the SAED pattern.

γ-Al_2O_3 nanopowders show the typical particle morphology with sharp edge, containing short rods and hexagons. SAED pattern in (d) displays two concentric rings assigned to the (004) and (044) crystal planes of γ-Al_2O_3, respectively.

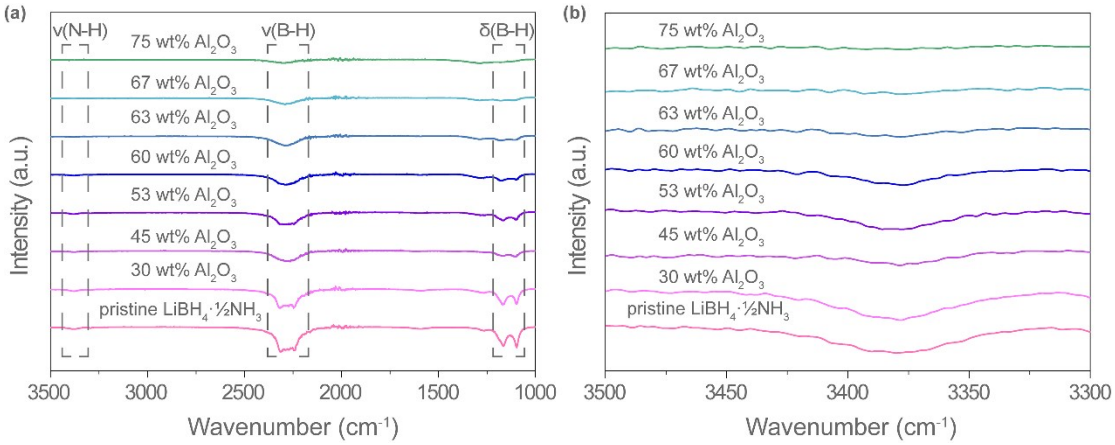

Fig. S2 (a) ATR-FTIR spectra of the $LiBH_4 \cdot ½NH_3$-Al_2O_3 composites with different amounts of Al_2O_3, compared with the pristine $LiBH_4 \cdot ½NH_3$ and (b) magnified curves of 3500－3300 cm^{-1} wavenumber on the part of N-H vibration.

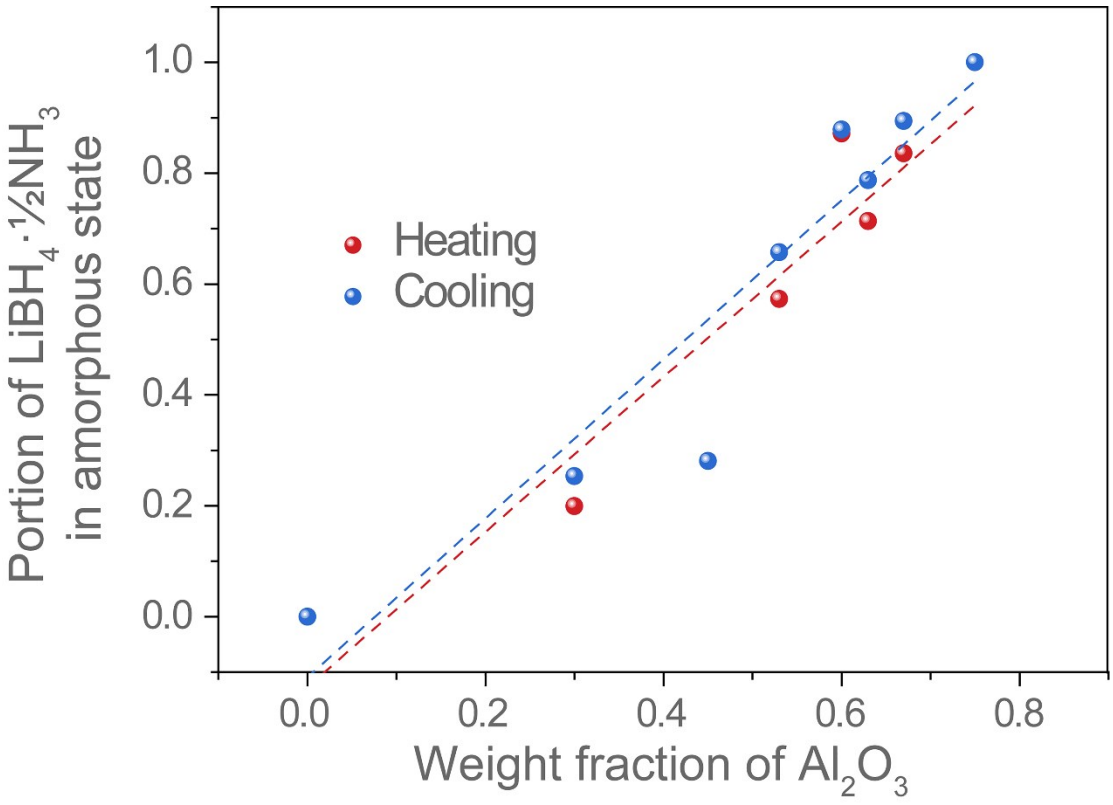

Fig. S3 Portion of $LiBH_4 \cdot ½NH_3$ in amorphous state of pristine $LiBH_4 \cdot ½NH_3$ and $LiBH_4 \cdot ½NH_3$-Al_2O_3 composites calculated in the heating/cooling process.

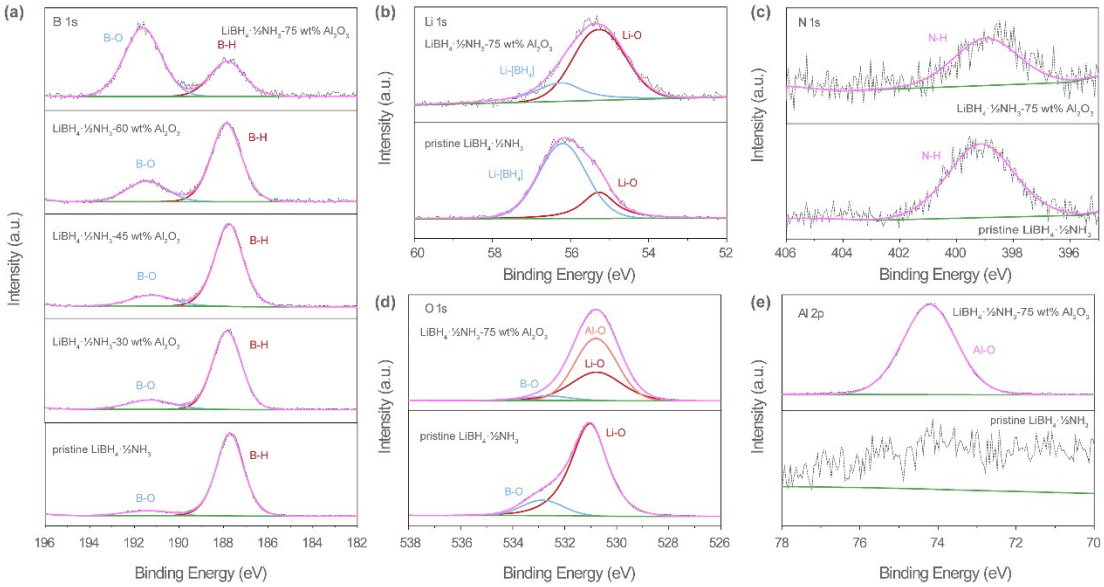

Fig. S4 (a) B 1s XPS spectra of $LiBH_4 \cdot ½NH_3$-Al_2O_3, (b) Li 1s, (c) N 1s, (d) O 1s and (e) Al 2p XPS spectra of $LiBH_4 \cdot ½NH_3$-75 wt% Al_2O_3 compared with the pristine $LiBH_4 \cdot ½NH_3$ without Al_2O_3 addition.

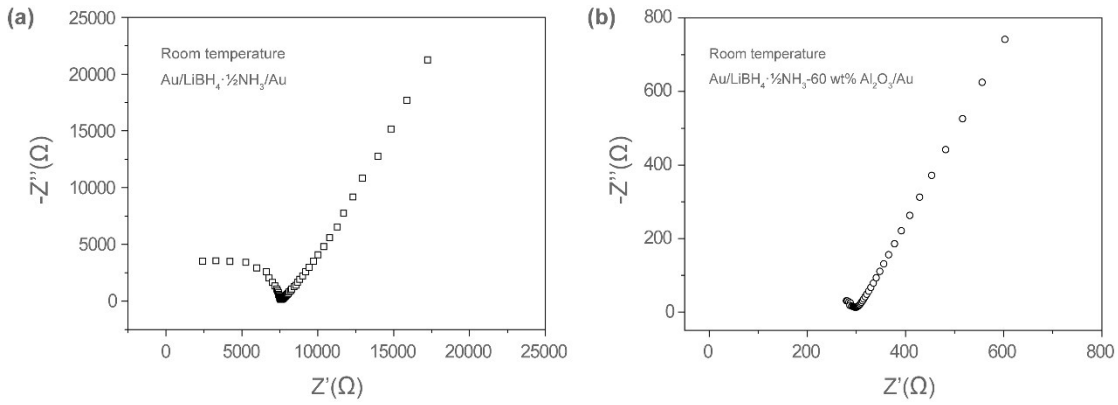

Fig. S5 Nyquist plots of (a) $LiBH_4 \cdot ½NH_3$ and (b) $LiBH_4 \cdot ½NH_3$-60 wt%Al_2O_3 at room temperature.

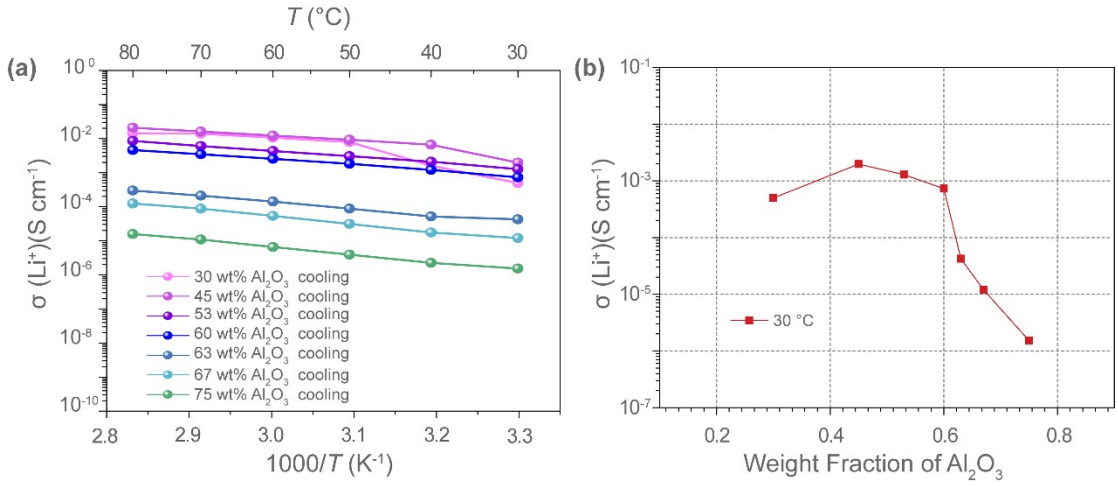

Fig. S6 (a) Temperature-dependent Li-ion conductivities and (b) Li-ion conductivities at 30 ºC of as a function of Al_2O_3 amount of the $LiBH_4 \cdot ½NH_3$-Al_2O_3 composite in cooling process.

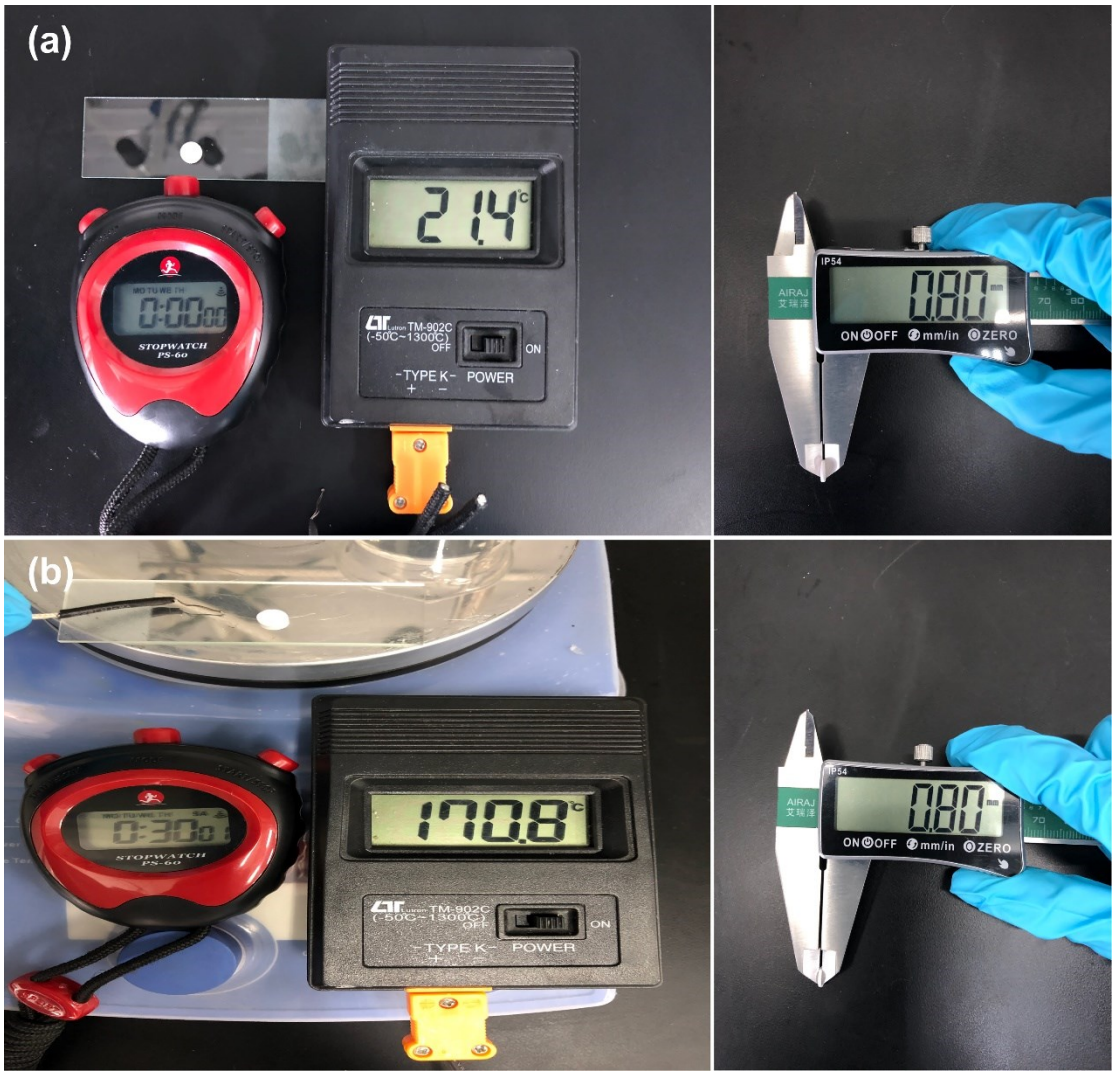

Fig. S7 Tests of a $LiBH_4 \cdot ½NH_3$-60 wt% Al_2O_3 pellet heated at 170 ºC for 0.5 h in air.